JOURNAL OF MAGNETIC RESONANCE **132,** 266–273 (1998)
ARTICLE NO. MN981413

A Six-Pulse PASS MAS-NMR Technique Solved by a Phasor Method

Birgit Effey,* J. A. Butcher, Jr.,† and R. L. Cappelletti*

*Condensed Matter and Surface Sciences Program: *Department of Physics and Astronomy and †Department of Chemistry, Ohio University, Athens, Ohio 45701*

Received May 20, 1997; revised January 28, 1998

The PASS MAS-NMR technique is capable of recovering full intensities of the central resonances of a spectrum by phase adjusting the spinning sidebands. This variant of the original PASS sequence by Dixon uses six π pulses instead of four. The addition of two π pulses provides more flexibility in choosing the spacing between pulses and therefore eliminates pulse overlap and receiver dead-time problems. The nonlinear, underdetermined PASS equations were solved using a graphical phasor method. All PASS sequences were successfully tested. A table of the six pulse delay times for different pitches is presented.

INTRODUCTION

Magic angle spinning (MAS) NMR (*1, 2*) averages the second-rank chemical shift tensor by rotating the sample about an axis inclined at a 54° 44′ angle (the ''magic angle'') with respect to the external magnetic field. This technique provides high-resolution NMR spectra of solids, with lineshapes comparable to those of solutions. Spinning the solid sample at the magic angle leads to a spectrum composed of a central peak at the isotropic shift of each resonance and additional spinning sidebands equally spaced at the rotor frequency from and in phase with the central peak (*3, 4*). Except for determination and analysis of the chemical shift tensor, spinning sidebands are rather unwelcome guests in a complex spectrum, since sidebands reduce the central peak intensity by an amount equivalent to their own intensities. Analyzing the spectrum of a compound with more than one resonance might result in the overlapping of central peaks and sidebands, both in general indistinguishable from each other, and therefore making quantitative, and even qualitative, interpretation difficult, if not impossible (*5, 6*). Sidebands are not observed at low magnetic fields or high spinning rates, because the frequency ν_r of the rotor exceeds that of the chemical shift anisotropy $\Delta\sigma$, expressed in Hz: $\nu_r > \Delta\sigma$. For NMR spectra, obtained under conditions not satisfying these criteria, other alternatives have to be found to solve the spinning-sideband problem. TOSS (*7–9*) is a special pulse sequence that totally suppresses spinning sidebands by time-averaging the magnetization trajectories from all crystallites in the sample during detection. Discarding the sidebands causes valuable chemical shift and intensity information to be lost (*3, 10*). Thus, except for the reduction of the number of peaks in a spectrum, sideband suppression is most undesirable. Two-thirds of the chemical shift information can be obtained from spinning sidebands by employing the intensity analysis of Herzfeld and Berger (*10*). A more sophisticated method, phase adjustment of spinning sidebands (PASS) (*7*), recovers the full intensities of the central resonance peaks and retrieves the information that is stored in the sidebands.

The six-pulse PASS sequence competes with various other solid-state NMR techniques. PASS is recommended for systems with short T_2 times, long T_1 times, and for experiments with long data acquisition. The newer 2D TOSS sequences (*11, 12*) are the two-dimensional analogue to PASS. They have the advantage that pure absorptive sideband lineshapes are obtained. On the other hand they require eight π and two $\frac{\pi}{2}$ pulses and about twice the time range of PASS (t_{PASS}), therefore reducing the magnetization by a multiplicative factor of $\sim e^{-2t_{PASS}/T_2}$, caused by transverse relaxation (T_2). This might lead to serious signal-to-noise problems for samples with short T_2 times. In addition, the signal of the 2D TOSS sequence is reduced further by a multiplicative factor of $2e^{-2t_r/T_2}$ compared to PASS because two scans (real and imaginary) are required, producing $\sqrt{2}$ times more noise (*15*). A second 2D TOSS experiment which recovers full intensities of the central peaks by accumulating a spectrum $S(\omega_1, t_2 = 0)$ was introduced by Bodenhausen (*13*). This technique might also exhibit problems for samples with short T_2 times. The six-pulse PASS technique fills in the missing space of a 1D experiment which is able to fully recover isotropic intensities with a shorter acquisition time compared to the aforementioned 2D techniques, opening the studies of compounds with shorter T_2 times. The 1D PASS experiment might be useful in fields such as two- and three-dimensional polymer orientation NMR experiments (*15*), where a high number of scans and long data accumulation times are necessary. Also in the area of glasses (e.g., Se type glasses (*14*)), long T_1 times of 15 min or more produce lengthy experiments. In those cases a 2D TOSS experiment increases the duration of data acquisition by a factor

1090-7807/98 $25.00

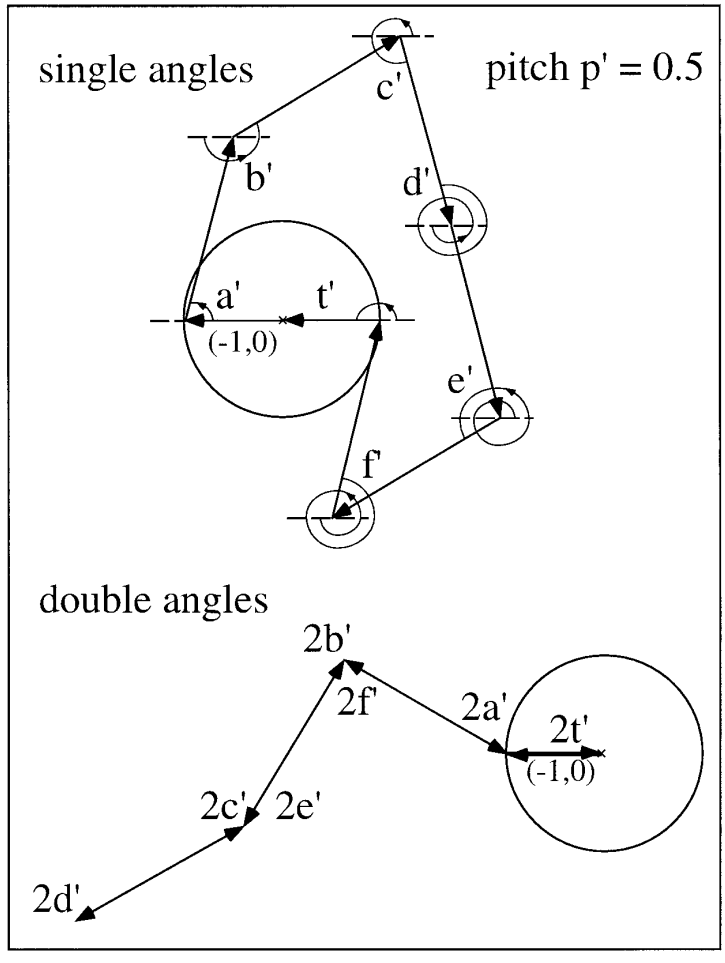

FIG. 1. One possible graphical solution of the two phasor diagrams for pitch $p = 0.5$ is displayed. Both phasor diagrams show a closed polygon train; for the double-angle diagram the phasors reverse their paths at the tip of the $2d'$ phasor. The indicated angles displayed in the top graph are omitted in the lower graph for clarity.

n, where n is the number of sidebands that need to be recovered (*11*). In contrast, PASS only requires two spectra to recover all even and all uneven sidebands, three spectra to recover all sidebands modulo 3, etc. (see Table 4).

The new PASS pulse sequence introduced in this publication uses six π pulses instead of only four. Pulse overlap and receiver dead-time problems prevent some of the pulse sequences in the original version of PASS from being implemented experimentally. The additional two π pulses eliminate these problems. The time between pulses is not shorter than one-tenth of a rotor period in the six π pulse sequence. Therefore, higher spinning rates are allowed. Assuming a 90° pulse having a pulse width (pw) of 10 μs for an upper limit, a spinning rate (srate) of 5000 Hz is allowed:

$$srate = \frac{0.1}{2pw} = \frac{0.1}{20\ \mu\text{s}} = 5000\ \text{Hz}. \qquad [1]$$

Solving the four transcendental PASS equations is more easily done graphically, rather than by a numerical approach. The latter involves the guess of initial conditions, the production of many divergent or unphysical results, and high CPU times. Presented next are the results obtained by using a graphical program as a ''virtual instrument,'' which runs within the LabVIEW[1] environment. The user is able to change and improve initial parameters, and with a little patience a solution is usually found within minutes.

THE SIX π PASS EQUATIONS

An excellent description of echo formation in solids is provided in Dixon's PASS paper (*7*). The following treatment extends the PASS equations to six π pulses. In order

[1] LabVIEW is a virtual instrument programming environment workbench available from National Instruments, Austin, Texas.

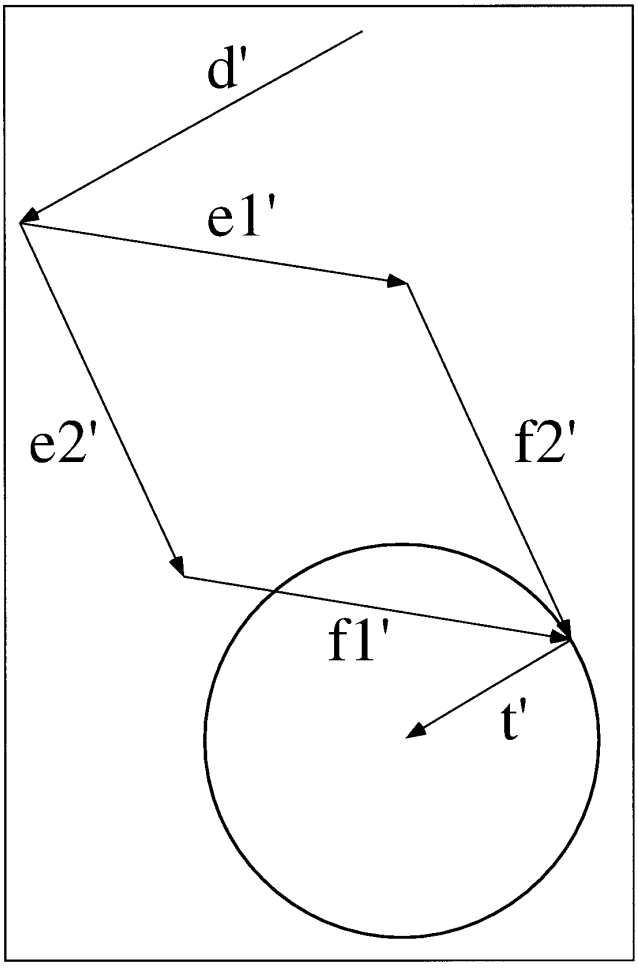

FIG. 2. An example of the two different solutions (e'_1, f'_1) and (e'_2, f'_2) that can be found by trying to connect the d' phasor with the tail of the t' phasor. The graphical program calculates the missing $e'_{1,2}$ and $f'_{1,2}$. This method ensures that the selected values always satisfy the single-angle equation [8].

to obtain an echo in a rotating solid the phases of all spins in the sample need to be refocused. This can be achieved by applying several π pulses. The expression for the phase of any spin after six π pulses leads to the four transcendental PASS equations.

$$\cos(t') = 1 - 2\cos(a') + 2\cos(b') - 2\cos(c') + 2\cos(d') - 2\cos(e') + 2\cos(f') \quad [2]$$

$$\sin(t') = -2\sin(a') + 2\sin(b') - 2\sin(c') + 2\sin(d') - 2\sin(e') + 2\sin(f') \quad [3]$$

$$\cos(2t') = 1 - 2\cos(2a') + 2\cos(2b') - 2\cos(2c') + 2\cos(2d') - 2\cos(2e') + 2\cos(2f') \quad [4]$$

$$\sin(2t') = -2\sin(2a') + 2\sin(2b') - 2\sin(2c') + 2\sin(2d') - 2\sin(2e') + 2\sin(2f') \quad [5]$$

where $a' = 2\pi a$ and $a = t_a/T_{rot}$. Then a is the delay time t_a for the first 180° pulse, expressed as a fraction of a rotor period. Analogous considerations can be applied to $b', \ldots f'$, and t'. For a given t, the six pulse times have to be chosen in a way that Eqs. [2]–[5] are satisfied.

Another important aspect of echo formation is the acquisition time. Eqs. [2]–[5] only calculate the pulse-delay times in order to achieve a rotational echo. A solid sample with two or more sites, having different chemical shifts and Larmor frequencies, restricts the freedom of choosing an arbitrary acquisition time. Since all spins, regardless of their different Larmor frequencies, should have the same phase at the time of acquisition (t_{acq}), digitizing has to be started according to the Hahn-echo condition:

$$t_{acq} = 2(f - e + d - c + b - a) = t - p, \quad [6]$$

where p is the ''pitch,'' expressed also as a fraction of the rotor period. The key to spinning-sideband manipulation is the delay of rotational echoes (*7*). A usual free induction decay (fid) starts with a maximum coherence, representing a rotational echo in the time domain. This fid contains terms of the form $e^{(imt')}$, where m is the order of the sideband: $m = \pm 1, \pm 2,$

TABLE 1
Pitch $p = n/8$ Delay Times for the Six π Pulses

a	*b*	*c*	*d*	*e*	*f*	Acquisition	Pitch
0.13021	0.50810	0.62331	0.74681	0.90968	1.09384	1.37100	0.125
0.22790	0.55010	0.65991	0.77459	0.95273	1.18129	1.33083	0.250
0.19701	0.29799	0.74525	1.26329	1.39127	1.68088	1.81726	0.375
0.20982	0.58478	0.79037	1.29020	1.58494	1.70995	1.99989	0.500
0.24176	0.54275	0.83174	1.30168	1.57543	1.73991	1.87083	0.625
0.10040	0.48471	0.59490	0.78139	0.88713	1.11616	1.59972	0.750
0.28201	0.51203	0.62595	0.78370	0.90199	1.28952	1.55063	0.875

Note. The times are in fractions of one rotor period.

TABLE 2
Pitch $p = n/12$ Delay Times for the Six π Pulses

a	*b*	*c*	*d*	*e*	*f*	Acquisition	Pitch
0.15722	0.53603	0.65189	0.77670	0.92418	1.13330	1.42553	0.0833
0.19695	0.54397	0.65740	0.77557	0.93812	1.16206	1.37817	0.1667
0.22790	0.55010	0.65991	0.77459	0.95273	1.18129	1.33083	0.2500
0.14434	0.35132	0.74385	1.17101	1.40828	1.68819	1.82819	0.3333
0.19991	0.31056	0.75850	1.27705	1.40907	1.68761	1.81554	0.4167
0.20982	0.58478	0.79037	1.29020	1.58494	1.70995	1.99989	0.5000
0.23012	0.52843	0.81873	1.29646	1.55629	1.73075	1.90087	0.5833
0.15756	0.38879	0.50284	0.73385	0.88874	1.02135	1.18963	0.6667
0.10040	0.48471	0.59490	0.78139	0.88713	1.11616	1.59972	0.7500
0.10095	0.49597	0.61457	0.78543	0.90051	1.10933	1.5494	0.8333
0.30959	0.57668	0.67729	0.81194	0.92188	1.31837	1.59647	0.9167

Note. The times are in fractions of one rotor period.

$\pm 3, \ldots . m = 0$ characterizes the central peak of that specific resonance. A modified fid starts at a time p either before or after the original fid, leading to the term

$$e^{im(t'+p')} = e^{imt'}e^{i\phi_m} \quad [7]$$

The additional term $e^{(i\phi_m)} = e^{(imp')}$ is the important phase change for each sideband of order m. Note that only the phases, not the amplitudes, of the sidebands are manipulated. The determination of the pulse delay and acquisition times for different pitches is discussed in the next section.

THE GRAPHICAL APPROACH

The PASS equations for the six π pulse sequence (Eqs. [2]–[5]) can be combined into two phasor equations:

$$e^{it'} - 1 + 2e^{ia'} - 2e^{ib'} + 2e^{ic'} - 2e^{id'} + 2e^{ie'} - 2e^{if'} = 0 \quad [8]$$

$$e^{2it'} - 1 + 2e^{2ia'} - 2e^{2ib'} + 2e^{2ic'} - 2e^{2id'} + 2e^{2ie'} - 2e^{2if'} = 0. \quad [9]$$

A solution is found whenever the time-dependent (the first terms) and time-independent parts of Eqs. [8] and [9] cancel each other. The graphical analogue would be that a solution is

TABLE 3
Pitch $p = n/20$ Delay Times for the Six π Pulses

a	*b*	*c*	*d*	*e*	*f*	Acquisition	Pitch
0.12926	0.53457	0.64839	0.77564	0.91704	1.10880	1.44864	0.05
0.16435	0.53787	0.65249	0.77564	0.92628	1.13814	1.41705	0.10
0.18800	0.54166	0.65526	0.77462	0.93452	1.15518	1.38736	0.15
0.20927	0.54639	0.65811	0.77459	0.94356	1.16969	1.35943	0.20
0.22790	0.55010	0.65991	0.77459	0.95273	1.18129	1.33083	0.25
0.24441	0.55262	0.66068	0.77457	0.96195	1.19058	1.30146	0.30
0.16687	0.33871	0.74403	1.20012	1.40248	1.68496	1.82094	0.35
0.19849	0.30930	0.75333	1.26587	1.40258	1.68507	1.81170	0.40
0.20417	0.31675	0.76946	1.31514	1.42477	1.69367	1.85433	0.45
0.20982	0.58478	0.79037	1.29020	1.58494	1.70995	1.99989	0.50
0.22268	0.50800	0.80688	1.29491	1.53013	1.72121	1.92886	0.55
0.23695	0.51593	0.82208	1.30150	1.54765	1.73081	1.88313	0.60
0.24686	0.56264	0.84119	1.30244	1.59841	1.74911	1.85545	0.65
0.12531	0.34373	0.46056	0.67744	0.79422	1.04013	1.36239	0.70
0.10040	0.48471	0.59490	0.78139	0.88713	1.11616	1.59972	0.75
0.13139	0.48887	0.60315	0.77919	0.89068	1.14166	1.56899	0.80
0.22758	0.50421	0.61817	0.78120	0.89704	1.23559	1.55641	0.85
0.29822	0.52418	0.63918	0.79103	0.90987	1.30366	1.54320	0.90
0.16847	0.54571	0.66464	0.80598	0.92540	1.16785	1.52205	0.95

Note. The times are in fractions of one rotor period.

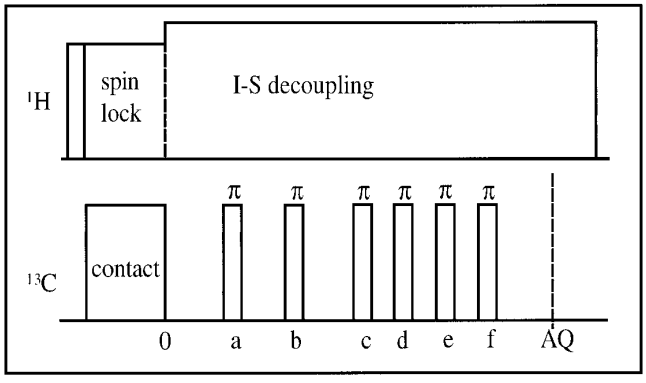

FIG. 3. The PASS sequence is based on a usual cross-polarization experiment, followed by six π pulses, which provide the phase adjustment of the sidebands.

reached whenever both equations simultaneously present closed polygon trains in their phasor diagrams. One possible graphical solution for pitch 0.5 is shown in Fig. 1.

This problem is solved graphically by using a virtual instrument[2] that runs within the LabVIEW environment. The user can solve the two phasor equations by adjusting the variables a', b', c', d', t' and the pitch p'. In addition, an indicator shows if the Hahn-echo constraint is satisfied. The program then calculates the missing e' and f' angles/phasors which provide a closed polygon train for the single-angle equation [8]. Either two or no (rarely one) solutions can be found (see Fig. 2). The two solutions are displayed as phasor diagrams on the screen. In addition the matching two double-angle phasor diagrams are shown. The goal is to choose the adjustable variables in such a way that one of the double-angle diagrams also closes its polygon train. On average, a solution that has the necessary accuracy (± 0.0001) for the PASS experiment can be reached within a few minutes by trial and error. The six pulse-delay times and the acquisition time for pitches p, which are integral multiples of $\frac{1}{8}$, $\frac{1}{12}$, and $\frac{1}{20}$, found by the phasor method described earlier, are listed in Tables 1, 2, and 3, respectively. This graphical approach should prove useful in solving similar NMR equations. The graphical solution addressed in this section was favored over our numerical attempts. Solving the four transcendental PASS equations numerically is difficult because the system is underdetermined with a complicated constraint (see Eq. [6]). With the guess of initial conditions, the production of many divergent or unphysical results, and high CPU times, numerical calculations did not yield a solution even after several days. We have not come across general analytical solutions to the PASS equations in the literature for arbitrary pitches. Compared to the analytical results of the TOSS equations (*19*, *20*), the PASS equations come with their additional variable, the pitch p. Even if analytical solutions for certain pitches exist, they are not likely to be experimentally useful.

[2] For further information on the graphical program, please contact the authors (e-mail: effey@helios.phy.ohiou.edu).

EXPERIMENTAL RESULTS AND DISCUSSION

The general pulse sequence is shown in Fig. 3. The pulse delay times for the six π pulses can be taken from Tables 1, 2, and 3. The time interval between pulses is measured from the centers of the pulses, suggesting that the π pulses must be kept as short as possible for the system to evolve freely between pulses. The phase cycling for the 180° pulses was an alternation between (x, y, x, y) and $(\bar{x}, \bar{y}, \bar{x}, \bar{y})$. To minimize pulse imperfection, composite pulses

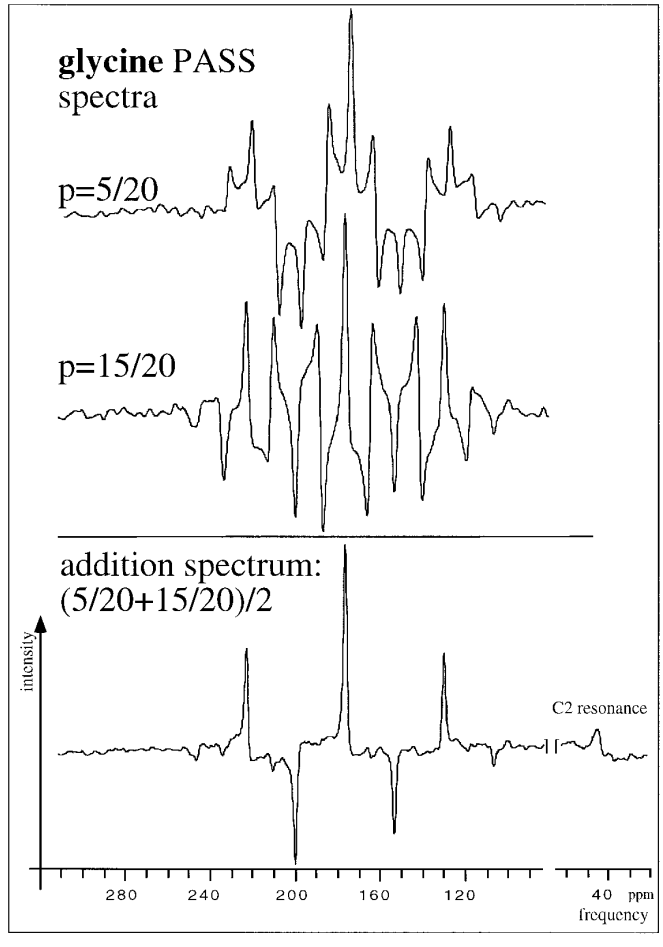

FIG. 4. PASS MAS-^{13}C NMR spectra of glycine with pitch $p = 5/20$ and 15/20 are presented. The data were taken on a 400-MHz Varian NMR VXR 5000, equipped with a Doty probe, with a spinning rate of 1224 ± 1 Hz. The duration of a 90° pulse for ^{13}C in the carboxylic acid group was determined to be 7.1 μs. The repetition time of the experiment was 5 s and 32 transients were taken for each spectrum. All odd sidebands can be suppressed by adding up the spectra $p = 5/20$ and 15/20. The C2 resonance of glycine, which is in phase with the isotropical peak of the C1 resonance, is shown for the addition spectrum. Chemical shifts are given in parts per million with respect to TMS.

TABLE 4
Addition Sequences for the PASS Spectra

±Sideband orders	Addition sequences
C_u, 2_u, 4_u, 6_u, etc.	$(6_{12} + 0)/2, \quad (10_{20} + 0)/2,$
C_u, 2_d, 4_u, 6_d, etc.	$(2_8 + 6_8)/2, \quad (3_{12} + 9_{12})/2, \quad (5_{20} + 15_{20})/2$
1_d, 3_d, 5_d, 7_d, etc.	$(4_8 - 0)/2, \quad (6_{12} - 0)/2, \quad (10_{20} - 0)/2,$
1_d, 3_u, 5_d, 7_u, etc.	$((1 - \sqrt{5})(2_{20} + 18_{20}) - (1 + \sqrt{5})(4_{20} + 16_{20} - 6_{20} - 14_{20}) - (1 - \sqrt{5})(8_{20} + 12_{20}) + 10_{20} - 0)/10$
C_u, 3_d, 6_u, etc.	$(2_{12} + 10_{12} + 6_{12})/3,$
C_u, 3_u, 6_u, etc.	$(4_{12} + 8_{12} + 0)/3,$
3_d, 6_u, 9_d	$-(1_{12} + 11_{12} + 3_{12} + 9_{12} + 4_{12} + 8_{12} + 5_{12} + 7_{12} + 0)/12 + (2_{12} + 10_{12} + 6_{12})/4,$
3_u, 6_u, 9_u	$-(1_{12} + 11_{12} + 2_{12} + 10_{12} + 3_{12} + 9_{12} + 5_{12} + 7_{12} + 6_{12})/12 + (4_{12} + 8_{12} + 0)/4$
C_u, 4_d, 8_u, etc.	$(1_8 + 7_8 + 3_8 + 5_8)/4,$ $((5 + 3\sqrt{5})(2_{20} + 18_{20} + 3_{20} + 17_{20} + 7_{20} + 13_{20} + 8_{20} + 12_{20}) - 2\sqrt{5}(1_{20} + 19_{20} + 4_{20} + 16_{20} + 6_{20} + 14_{20} + 9_{20} + 11_{20}))/(10(5 + \sqrt{5})) + (5_{20} + 15_{20} + 10_{20} + 0)/20,$
C_u, 4_u, 8_u, etc.	$(2_8 + 6_8 + 4_8 + 0)/4$
C_u, 5_u, 10_u	$(4_{20} + 16_{20} + 8_{20} + 12_{20} + 0)/5,$
C_u, 5_d, 10_u	$(2_{20} + 18_{20} + 6_{20} + 14_{20} + 10_{20})/5$
C_u, 6_u, 12_u, etc.	$(2_{12} + 10_{12} + 4_{12} + 8_{12} + 6_{12} + 0)/6,$
C_u, 6_d, 12_u, etc.	$(1_{12} + 11_{12} + 3_{12} + 9_{12} + 5_{12} + 7_{12})/6,$
6_u	$(-1_{12} - 11_{12} + 2_{12} + 10_{12} - 3_{12} - 9_{12} + 4_{12} + 8_{12} - 5_{12} - 7_{12} + 6_{12} + 0)/12$
C_u, 8_u	$(1_8 + 7_8 + 2_8 + 6_8 + 3_8 + 5_8 + 4_8 + 0)/8$
C_u, 10_u	$(2_{20} + 18_{20} + 4_{20} + 16_{20} + 6_{20} + 14_{20} + 8_{20} + 12_{20} + 10_{20} + 0)/10,$
C_u, 10_d	$(1_{20} + 19_{20} + 3_{20} + 17_{20} + 5_{20} + 15_{20} + 7_{20} + 13_{20} + 9_{20} + 11_{20})/10$
C_u, 12_u	$(1_{12} + 11_{12} + 2_{12} + 10_{12} + 3_{12} + 9_{12} + 4_{12} + 8_{12} + 5_{12} + 7_{12} + 6_{12} + 0)/12$

Note. The first column indicates the sideband orders to be recovered. Subscript *u* refers to having the sidebands in phase, and subscript *d* 180° out of phase, with respect to the central peak *C*. The right column displays the appropriate PASS sequences, labeled by their pitches (p), which must be added or subtracted in order to regain the selected sidebands. The pitch labels should be interpreted as follows: $p = 2/12$ is abbreviated 2_{12}. The usual spectrum, all sidebands in phase with the central peak, is simply labeled 0. The coefficients in the addition sequence are chosen to normalize the recovered sidebands to those of the 0 spectrum.

90_ϕ $180_{\phi\pm90°}$ 90_ϕ (*16*) were implemented into the PASS sequence. The disadvantage that comes with composite pulses is that the free evolution time between pulses is reduced and there-

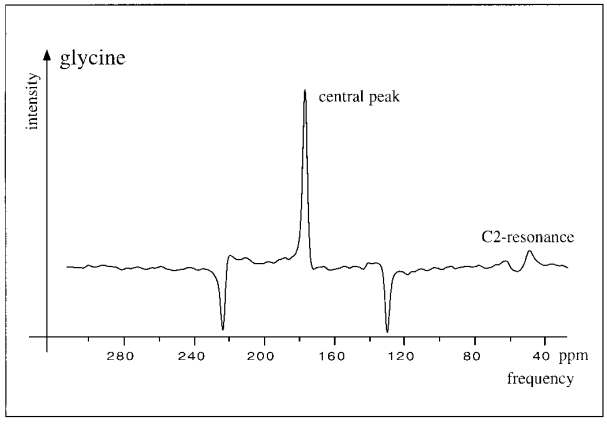

FIG. 5. This complex pulse addition sequence (the second term, row 9 of Table 4) recovers only sidebands ± 4. Chemical shifts are given in parts per million with respect to TMS.

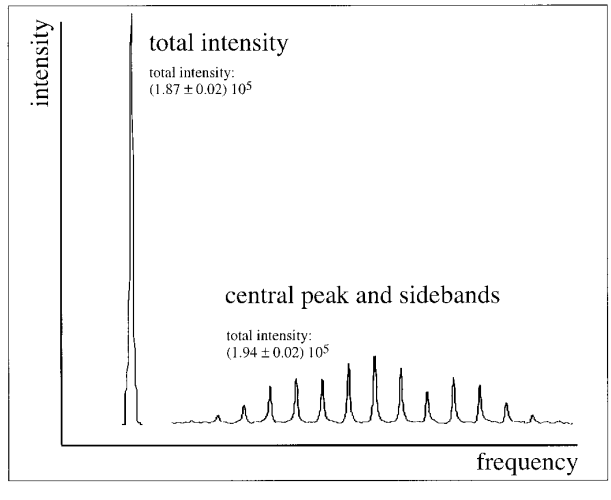

FIG. 6. The total intensity of the ^{13}C in the carboxylic acid group, which was obtained by shifting the recovered PASS sidebands into the central peak, is compared to the intensity distribution of this same resonance, spread over central peak and sidebands (see spectrum at right). A 4% deviation of the two intensities was found experimentally.

TABLE 5

CSA Values for the C1 Resonance of Glycine Determined via Herzfeld–Berger, Using Recovered Sideband Intensities from PASS Spectra

σ_{iso} (ppm)	σ_{11} (ppm)	σ_{22} (ppm)	σ_{33} (ppm)	Reference
177	247 ± 6	177 ± 1	109 ± 4	PASS recovered intensities
177	247	182	103	(*23*)
177	248	177	106	(*23*)
180	251	183	107	(*23*)

fore the maximum value for the spinning rate is decreased by a factor of 2. A more extended discussion of experimental problems can be found in Griffin's paper (*17*).

The six π PASS sequence was tested on a 400-MHz Varian VXR 5000, equipped with a Doty probe. ^{13}C NMR (100 MHz) was performed on glycine. Chemical shifts are given in parts per million with respect to TMS. The ^{13}C in the carboxylic acid group, which provides very narrow sidebands, was selected to examine PASS. The 180° pulses had a duration of 14.2 μs. A spinning rate of 1224 ± 1 Hz was chosen. The spinning rate was regulated to within ±1 Hz by a frequency controller made ''in-house'' (comparable to the one described in Ref. (*18*)). This level of accuracy is sufficient for the successful addition of spectra. Cross polarization was used to enhance sensitivity. Some selected spectra of glycine with pitches $p = 5/20$ and 15/20 are shown in Fig. 4. A variety of addition processes can be performed on the PASS spectra, cancelling chosen sidebands. Table 4 gives a small selection of spectral addition sequences that are useful in regaining the full intensity of the central peak. An example of the suppression of all odd sidebands (the third term, row 2 of Table 4), by adding up the $p = 5/20$ and 15/20 spectra, is shown in Fig. 4 (bottom spectrum), leaving the two isotropical resonances of glycine in phase with each other. However, the intensities of the C1 and C2 resonances are distorted because of cross-polarization effects. A more complex addition sequence (the second term, row 9 of Table 4) is shown in Fig. 5, illustrating the capabilities of PASS. Finally, in Fig. 6 the total intensity of the ^{13}C peak, obtained by shifting the isolated mth-order sidebands by $\pm m\nu_r$ into the central peak, is shown. Also, the standard MAS spectrum, which should have this same intensity spread over central peak and sidebands, is displayed to the right. Experimentally the two intensities were determined to $(1.87 \pm 0.02)10^5$ and $(1.94 \pm 0.02)10^5$, respectively, an indication of the quality of the procedure. Furthermore, the recovered sideband intensities were used to calculate the CSA of the C1 resonance of glycine via Herzfeld–Berger analysis. The results are listed next to literature values in Table 5. Our determined values are within the error limit of several published glycine CSAs.

CONCLUSIONS

Prior to this work, the only published PASS sequence was based on four π pulses (*7*). Experimental problems are pulse overlap and receiver dead-time in the delays of phase-altered spinning sidebands. Overlap can be eliminated by adding a rotor period between pulses which delays acquisition time by two rotor periods. This might lead to a severe decrease in the signal intensity, especially for samples with short T_2 times. By using six instead of four π pulses these problems are eliminated completely. Six adjustable parameters add more flexibility in choosing the spacing between pulses which permits higher spinning rates. Additionally, the acquisition time can be kept below 2.0 rotor periods. No receiver dead-time problems occur under these conditions. The PASS equations were solved using a graphical phasor solution rather than a numerical calculation. The LabVIEW program used can run on a PC. This approach might be helpful not only for PASS equations, since in general pulse sequences for solid-state NMR look rather similar to each other and can be solved using similar techniques. PASS might have future applications in the area of polymer and glass solid-state NMR experiments. PASS NMR experiments on glycine show that, by the addition of sequences, selected sidebands can be recovered and a linear phase shift across the spectrum can be avoided. The total intensity of the central peak can be obtained by adding all sidebands and central peak intensities together. Further, the isolated PASS sidebands can be used to calculate the chemical shift tensor by the Herzfeld and Berger analysis.

ACKNOWLEDGMENTS

This work was partially supported by the Condensed Matter and Surface Science Program of Ohio University and by NSF under Grant No. DMR 9604921. We would like to thank T. W. Dixon for insightful discussions about PASS, J. Liu for technical advice, M. M. Schwickert for significant help in designing the frequency controller and in developing the LabVIEW virtual instrument to solve the PASS equations, and H. Guerrero for his contributions to setting up a numerical attempt to solve the PASS equations.

REFERENCES

1. E. R. Andrew, A. Bradbury, and R. G. Eades, *Nature* **182,** 1659 (1958).
2. I. J. Lowe, *Phys. Rev. Lett.* **2,** 285 (1959).
3. M. M. Maricq and J. S. Waugh, *J. Magn. Reson.* **55,** 3300 (1979).
4. M. H. Levitt, *J. Magn. Reson.* **82,** 427 (1989).
5. P. F. Barron and M. A. Wilson, *Nature (London)* **289,** 275 (1981).
6. W. Aue, D. J. Ruben and R. G. Griffin, *J. Magn. Reson.* **43,** 472 (1981).
7. W. T. Dixon, *J. Chem. Phys.* **77,** 1800 (1982).
8. D. P. Raleigh, E. T. Olejniczak, and R. G. Griffin, *J. Chem. Phys.* **89,** 1333 (1988).

9. D. P. Raleigh, E. T. Olejniczak, S. Vega, and R. G. Griffin, *J. Magn. Reson.* **72,** 238 (1987).

10. J. Herzfeld and A. E. Berger, *J. Chem. Phys.* **73,** 6021 (1980).

11. S. F. De Lacroix, J. J. Titman, A. Hagemeyer, and H. W. Spiess, *J. Magn. Reson.* **97,** 435 (1992).

12. H. Geen and G. Bodenhausen, *J. Chem. Phys.* **97,** 2928 (1992).

13. H. Geen and G. Bodenhausen, *J. Am. Chem. Soc.* **115,** 1579 (1993).

14. H. Eckert, *Progress in NMR Spectroscopy* **24,** 159 (1992); R. Maxwell, H. Erickson, and H. Eckert, *Z. Naturforsch.* **50a,** 395 (1994); R. Maxwell, D. Lathrop, D. Franke, and H. Eckert, *Angew. Chem. Int. Ed. Engl.* **29,** 882 (1990).

15. K. Schmidt-Rohr and H. W. Spiess, ''Multidimensional Solid State NMR and Polymers,'' p. 204. Academic Press, San Diego (1994).

16. M. H. Levitt and R. Freeman, *J. Magn. Reson.* **33,** 473 (1979).

17. D. P. Raleigh, A. C. Kolbert, and R. G. Griffin, *J. Magn. Reson.* **89,** 1 (1990).

18. T. D. Maier and T. Huang, *J. Magn. Reson.* **91,** 165 (1991).

19. Z. Song, O. N. Antzutkin, X. Feng, and M. H. Levitt, *Solid State Nucl. Magn. Reson.* **2,** 143 (1993).

20. O. N. Antzutkin, Z. Song, X. Feng, and M. H. Levitt, *J. Chem. Phys.* **100,** 130 (1994).

21. T. M. Duncan, ''Compilation of Chemical Shift Tensors,'' Farrugot Press, Chicago (1996).